Miner Deposita (2006) 40: 849–866
DOI 10.1007/s00126-005-0037-3

ARTICLE

Edson F. Mello · Roberto P. Xavier · Neal J. McNaughton · Steffen G. Hagemann · Ian Fletcher · Larry Snee

Age constraints on felsic intrusions, metamorphism and gold mineralisation in the Palaeoproterozoic Rio Itapicuru greenstone belt, NE Bahia State, Brazil

Received: 24 February 2004 / Accepted: 22 November 2005 / Published online: 21 January 2006

Abstract U–Pb sensitive high resolution ion microprobe mass spectrometer (SHRIMP) ages of zircon, monazite and xenotime crystals from felsic intrusive rocks from the Rio Itapicuru greenstone belt show two development stages between 2,152 and 2,130 Ma, and between 2,130 and 2,080 Ma. The older intrusions yielded ages of 2,152±6 Ma in monazite crystals and 2,155±9 Ma in zircon crystals derived from the Trilhado granodiorite, and ages of 2,130±7 Ma and 2,128±8 Ma in zircon crystals derived from the Teofilândia tonalite. The emplacement age of the syntectonic Ambrósio dome as indicated by a 2,080±2-Ma xenotime age for a granite dyke probably marks the end of the felsic magmatism. This age shows good agreement with the Ar–Ar plateau age of 2,080±5 Ma obtained in hornblendes from an amphibolite and with a U–Pb SHRIMP age of 2,076±10 Ma in detrital zircon crystals from a quartzite, interpreted as the age of the peak of the metamorphism. The predominance of inherited zircons in the syntectonic Ambrósio dome suggests that the basement of the supracrustal rocks was composed of Archaean continental crust with components of 2,937±16, 3,111±13 and 3,162±13 Ma. Ar–Ar plateau ages of 2,050±4 Ma and 2,054±2 Ma on hydrothermal muscovite samples from the Fazenda Brasileiro gold deposit are interpreted as minimum ages for gold mineralisation and close to the true age of gold deposition. The Ar–Ar data indicate that the mineralisation must have occurred less than 30 million years after the peak of the metamorphism, or episodically between 2,080 Ma and 2,050 Ma, during uplift and exhumation of the orogen.

Keywords SHRIMP U–Pb geochronology · Ar–Ar dating · Trans-Amazonian cycle · Gold metallogeny · Rio Itapicuru greenstone belt · São Francisco Craton · Brazil

Editorial handling: F. Tornos

Electronic Supplementary Material Supplementary material is available for this article at http://dx.doi.org/10.1007/s00126-005-0037-3

E. F. Mello (✉)
Departamento de Geologia, Instituto de Geociências,
Centro de Ciências Matemáticas e da Natureza,
Universidade Federal do Rio de Janeiro (UFRJ),
Av Brigadeiro Trompowski, s/n, Cidade Universitária,
Ilha do Fundão, Rio de Janeiro,
21949-900, Brazil
e-mail: mello@geologia.ufrj.br
Tel.: +55-021-25989464
Fax: +55-021-25989465

R. P. Xavier
Instituto de Geociências,
Universidade Estadual de Campinas (Unicamp),
Campinas, SP, Brazil

N. J. McNaughton · S. G. Hagemann · I. Fletcher
Centre for Global Metallogeny,
Department of Geology and Geophysics,
University of Western Australia,
Nedlands, 6907, Australia

L. Snee
U.S. Geological Survey,
M.S., Denver Federal Center, Box 25046,
Denver, CO 80225, USA

Introduction

The Rio Itapicuru greenstone belt (RIGB) is the largest and the most economically important Palaeoproterozoic granite–greenstone terrain in the northeast portion of the São Francisco Craton, a major geotectonic unit in the eastern part of the South American Platform (Fig. 1). The São Francisco Craton, Guyana Shield, West Africa Craton and Congo Craton, show similar patterns of crustal development from 2.25 to 2.00 Ga, indicating that the Transamazonian Orogeny in South America probably correlates to the Eburnean Orogeny in Africa. The evolutionary similarities of these crustal segments is characterised by greenstone belts and associated plutons followed by a period of deformation associated with voluminous sedimentation, emplacement of syn- to late-tectonic plutons in the volcanic belts and finally intrusion of later syntectonic and sinmetamorphic plutons in the sedimentary basins

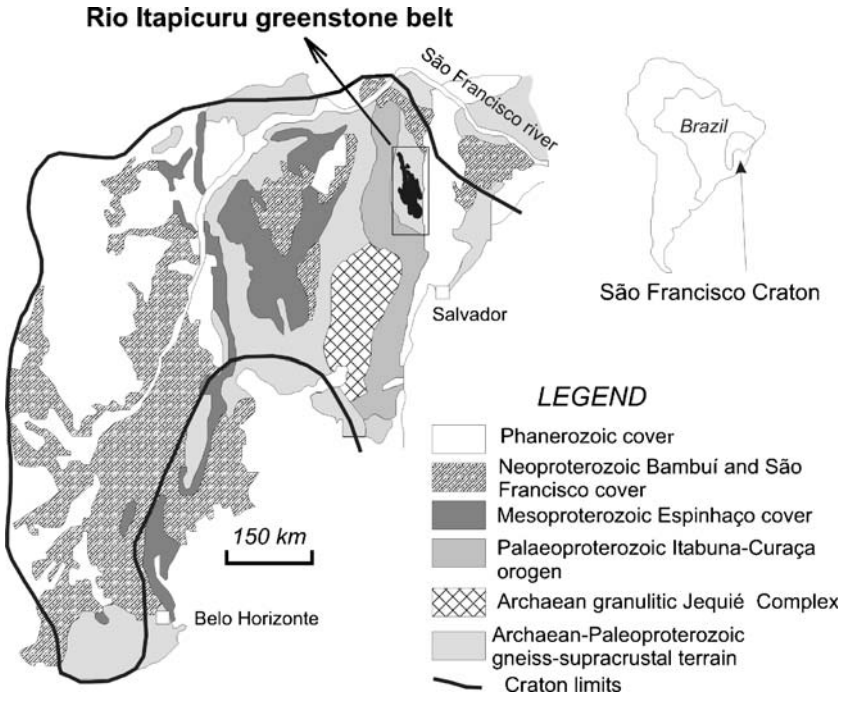

Fig. 1 Location of the Rio Itapicuru greenstone belt in northern Brazil, within the São Francisco Craton (Oliveira et al. 2002)

(Taylor et al. 1992; Abouchami et al. 1990; Boher et al. 1992; Davis et al. 1994; Feybesse and Milési 1994; Feybesse et al. 1998; Hirdes and Davis 2002; Hirdes et al. 1992, 1996; Ledru et al. 1994; Zhao et al. 2002; Hartmann 2002; Delor et al. 2003).

Age determinations on the mineralisation and several key rock units in the Guyana Shield and the West Africa Craton have established a framework for the timing of gold mineralisation and are broadly in agreement with similar rocks dated elsewhere (Oberthür et al. 1998; Norcross et al. 2000; Milési et al. 2003). The high gold potential of the Palaeoproterozoic terranes in South America and West Africa has attracted attention to correlations between these terrains.

The economic importance of the RIGB resides on the occurrence of several small-to medium-sized, shear zone-hosted lode gold deposits (i.e. orogenic type; Groves et al. 1998) in its southern (Weber Belt) and northern central sectors (Fig. 2).

Several regional and deposit scale studies developed over the last two decades have defined the major lithological and structural controls (Montes Lopes 1982; Marimon et al. 1986; Teixeira et al. 1990; Reinhardt and Davison 1990; Melo 1990; Xavier and Foster 1991; Alves da Silva and Matos 1991), the nature of the mineralising fluids and the P–T conditions of the mineralisation environment (Xavier 1987; Xavier and Foster 1991; Xavier et al. 1994; Coelho 1994). As a consequence of these studies, a deep-seated CO_2-rich, low-salinity aqueous fluid regime was incorporated as a major component of the proposed model for the RIGB gold mineralisation, similar to those for orogenic gold deposits all over the world (Teixeira 1985; Reinhardt and Davison 1990; Xavier 1991; Xavier et al. 1994). However, the question of the timing of infiltration of this mineralising fluid regime in relation to the regional metamorphism and felsic magmatism remained speculative (Xavier et al. 1994).

The major goal of this study, employing U–Pb sensitive high resolution ion microprobe mass spectrometer (SHRIMP) dating techniques, is to determine the ages of the felsic intrusives and metamorphism of the RIGB, and to constrain the age of gold mineralisation by dating sinmineralisation micas by the Ar–Ar technique. For the latter, the Fazenda Brasileiro deposit, in the southern sector, was taken as a case study because it is the largest and most productive within the RIGB and its geology has been extensively investigated (Montes Lopes 1982; Marimon et al. 1986; Xavier 1987; Teixeira et al. 1990; Reinhardt and Davison 1990; Melo 1990; Xavier and Foster 1991; Alves da Silva and Matos 1991; Coelho 1994).

Regional geology and geodynamic evolution

The RIGB consists of volcanic sedimentary rocks represented from bottom to top by a succession of (1) tholeiitic basalts with intercalated chemical sedimentary rocks; (2) andesites, dacites and rhyodacites interbedded with pyroclastics; and (3) volcanic greywackes and pelites, with subordinate arkoses, conglomerates and chemical sediments (Fig. 2) (Kishida and Riccio 1980; Silva 1984). This volcano-sedimentary sequence is intruded mainly by elliptical-shaped, granite-gneiss domes of granodiorite to tonalite composition, in general with a calc-alkaline affinity, and gabbroic sills (Kishida and Riccio 1980; Silva 1987). Regional metamorphism is greenschist facies, except near the edges of the granite–gneiss domes where the supracrustals are metamorphosed to amphibolite facies (Silva 1984).

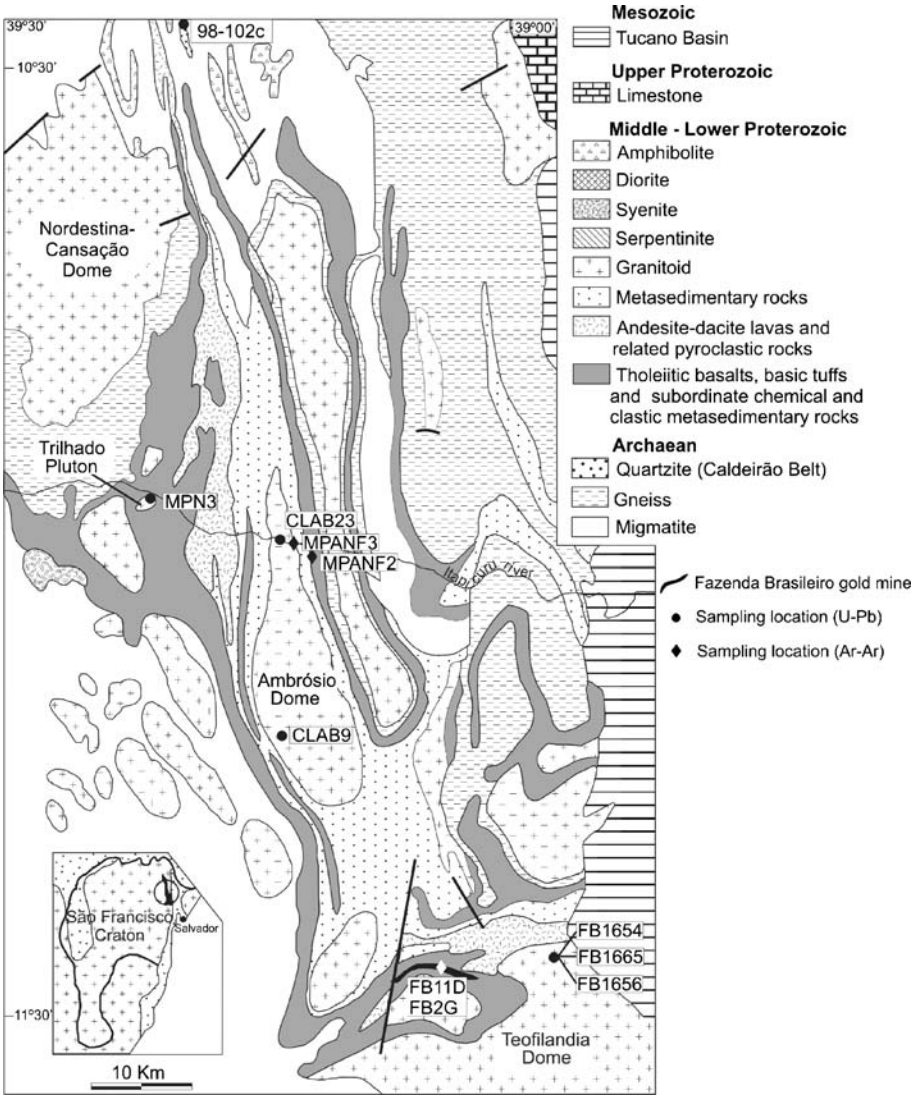

Fig. 2 Geological map of the Rio Itapicuru greenstone belt and sample location. (Modified from Rocha Neto 1994)

The structural feature commonly observed in the supracrustal rocks is characterised by a succession of large synclines and anticlines delimited by regional-scale, brittle–ductile shear zones, with a general N–S orientation, for the most part of the greenstone belt, and E–W to NW–SE in the southern sector (Kishida and Riccio 1980; Alves da Silva 1994). These structures have been related to a D2 deformation event, by far the most prominent in the region, during which the bulk of the felsic intrusives were emplaced (Matos and Davison 1987; Davison et al. 1988; Alves da Silva 1994). Post-D2 intrusions are subordinate and refer to some rounded to slightly ellipsoidal isotropic bodies of granodiorite composition, which occur enclosed in the mafic volcanic rocks (Silva 1984, 1992) and in the gneiss–migmatite basement located west of the supracrustal rocks, near the boundary of the granite–greenstone terrains and the Salvador-Curaçá mobile belt (Burgos et al. 1999; Peixoto et al. 1999).

The geodynamic model for the RIGB considers the evolution of a volcanic arc and its corresponding back-arc basin, developed on a sialic crust, in the transition from the Archaean to the Lower Proterozoic (Silva 1987). The set of geochronological data available for the RIGB, compiled in Table 1, reveals that the evolution of this belt took place mainly in the 2,200–2,030 Ma interval.

The beginning of the eruptive activity is dated by metabasalt whole rock ages of 2,209±60 Ma (2σ, Pb/Pb isochronic) and 2,200 Ma (Sm/Nd model age), whereas the subsequent felsic volcanism was probably active between 2,178±12 Ma (Pb–Pb, isochron) (Gáal et al. 1987 unpublished data) and 2,100 Ma (Sm/Nd whole rock) (Silva 1992). The closure of the Palaeoproterozoic basin was marked by intense plutonic activity in the interval of 2,127±5 Ma (1σ) and 2,079±47 Ma (2σ), recorded by the emplacement of the Barrocas, Ambrósio, Poço Grande, Santa Luz and Nordestina-Cansanção domes (Alves da Silva 1994; Chauvet et al. 1997). Late- to post-collisional magmatism, within the context of the compressive events in the RIGB, has been constrained by Pb–Pb ages of 2,067±22 and 2,086±17 Ma, respectively, for the Morro das Agulhas and Morro das Bananas syenites (Burgos et al. 1999) and by a Pb–Pb age of 2,003±2 Ma obtained for the Morro do

Table 1 Geochronological data from the Rio Itapicuru greenstone belt

Lithology	Method	Sample	Age (Ma)	$^{87}Sr/^{86}Sr_i$	ε_{Nd}	μ_1	MSWD	Reference
Gneiss	U–Pb	Zr	2930±32					3
Migmatite	K–Ar	Biot	2029±91					2
Amphibole-Gneiss	K–Ar	Hornb	2250±110					2
Granite-Gneiss	K–Ar	Biot	722±36					2
Metatexite	K–Ar	Biot	2040					2
		Musc	2012					2
Metabasalt	Sm–Nd	WR	2200		+4			5
	Pb–Pb	WR	2209±60			8.14	1.5	5
	Sm–Nd	WR	2100		+2			5
	Pb–Pb	WR	2109±80			8.0	2.0	5
	Pb–Pb (Isochron)	Ep, Ap, Zr	2178±12					3
	Rb–Sr	WR	2080±90(Ref)	0.7017			1.03	2
Metaandesite	Rb–Sr	WR	1642±312					2
	Rb–Sr	WR	1761±108					2
	Rb–Sr	WR	1998±155	0.705				2
	Rb-Sr	WR	1963±120					2
	Rb–Sr	WR	1927±95					2
	K–Ar	WR	1956±45					2
	K–Ar	WR	2084±45					2
Cansanção Monzonite	Rb–Sr	WR	2025±47	0.703			0.74	4
	Pb–Pb (evp)	Zr	2105±3					7
Nordestina Granodiorite	Rb–Sr	WR	2114±103	0.705				2
	Sm–Nd	WR	2400		−3			4
	Pb–Pb (evp)	Zr	2100±10					1
Barrocas Granodiorite	Pb–Pb (evp)	Zr	2127±5					1
	Ar–Ar	Biot	2029±13					1
Poço Grande Granite	Ar–Ar	Musc	2023±13					1
	U–Pb	Zr e Mz	2079±47					3
Santa Luz Granite	U–Pb	Zr	2107±23					3
	Rb–Sr	WR	2092±72	0.705				2
	Rb–Sr	WR	2146±97	0.705				2
	K–Ar	Biot	1790					2
	K–Ar	Biot	1791±53					2
Araci Granite	Rb–Sr	WR	2054±60					2
Ambrósio Pegmatite	Rb–Sr	WR	2030±58					1
	Rb–Sr	WR	2015±59					1
	Rb–Sr	WR	2000±60					1
Morro das Agulhas Syenite	Pb–Pb (evp)	Zr	2067±22					6
Morro das Bananas Syenite	Pb–Pb (evp)	Zr	2086±17					6
Morro dos Afonso Syenite	Pb–Pb (evp)	Zr	2098±9					8
	Pb–Pb (evp)	Zr	2081±27					8
Morro dos Lopes Granite	Pb–Pb (evp)	Zr	2003±2					9

1, Alves da Silva 1994; 2, Brito Neves et al. 1980; 3, Gáal et al. 1987 unpublished data; 4, Sabaté et al. 1990; 5, Silva 1992; 6, Burgos et al. 1999; 7, Oliveira et al. 1999; 8, Rios et al. 1999; Peixoto et al. 1999

Ref Reference isochron, *evp* evaporation, *WR* Whole Rock, *Zr* zircon, *Mz* monazite, *Musc* muscovite, *Biot* biotite, *Ep* epidote, *Ap* apatite, *Horn* hornblende

Lopes (Peixoto et al. 1999) granite, all of them in the western border of the greenstone belt.

The geochronological data for the gold mineralisation available up to now are restricted to apparent Ar–Ar ages obtained in muscovite and biotite crystals from the mineralised zone of the Fazenda Brasileiro deposit (Vasconcelos and Becker 1992). The muscovite provided an age of 2,049±4 Ma and biotite indicated an interval between 2,083±4 and 2,031±4 Ma.

The Archaean gneissic–migmatitic rocks of the basement occur east and west of the RIGB and a set of clastic and chemical metasedimentary rocks in structural conformity with Archaean polydeformed rocks occur in the northern segment of the RIGB. This last rock association

extends in a N–S direction for approximately 120 km forming the Caldeirão belt consisting of fuchsite-bearing quartzites, metapelites, migmatites, deformed granitoids and mafic rocks, all of which exhibit amphibolite facies mineral parageneses (Oliveira et al. 2002; Mello et al. 1999).

The Fazenda Brasileiro gold deposit

In the southern sector of the RIGB lies the most economically important gold deposit, Fazenda Brasileiro, with underground proved reserves of 1,936,000 t at 2.90 g/t of sulphide ore (Yamana Gold INC, 2005, personal communication). The total of gold production at the end of 2003 was more than 66.9 tonnes (Yamana Gold INC 2005). Other deposits in the RIGB, with operations presently suspended, have contributed with less than 25% of the total gold production of the belt.

The mineralised zone at the Fazenda Brasileiro deposit extends for 8 km surrounding the Barrocas granodiorite dome, along a 200-m thick, E–W-striking shear zone, dipping 45 to 60°S (Fig. 2) (Reinhardt and Davison 1990). The major orebodies consist of sulfide-rich, quartz–carbonate–albite vein systems hosted by a quartz–carbonate–chlorite schist, interpreted as a hydrothermally-altered mafic intrusion (Teixeira et al. 1990), and subordinately, by carbonaceous metapelites. The alteration assemblage generally present in the vicinity of the gold-bearing vein systems includes quartz + albite + carbonate ± biotite ± sphene + ilmenite + rutile + sulfides (mainly arsenopyrite, pyrrhotite and minor pyrite) (Marimon et al. 1986).

The gold-bearing vein system comprises single tabular veins or may form sets of intersecting veins, similar to a stockwork. As shown in Fig. 3, they are grouped into six distinct types (Mello et al. 1996):

1. Type I: breccia-like, 0.5 up to 4 m thick, irregular masses, concordant with the foliation (E–W/45–50°S)
2. Type II: foliation concordant, centimetre-thick, folded and boudinaged veins
3. Type III: centimetre-thick "*en echelon*" veins, parallel to the E–W striking foliation, but dipping north
4. Type IV: NW–SE-striking, 0.3 up to 0.5 m thick, subvertical veins
5. Type V: E–W-striking, dipping 25 to 45°N, breccia vein, which may extend for over 600 m along strike
6. Type VI: centimetre-thick, N–S-striking discordant veins, generally barren

The interpreted paragenetic sequence of the alteration and vein mineralogy is shown in Fig. 4.

On the basis of fluid inclusion studies, two main types of ore fluids were broadly associated with the gold mineralisation at the Fazenda Brasileiro deposit: a CO_2 ± (CH_4 + N_2) fluid and a low salinity (<6 wt.% eq. NaCl) H_2O–CO_2–(± CH_4 ± N_2) fluid (Xavier et al. 1994). On the basis of stable isotope data, these fluids were interpreted, as part of a deep hydrothermal system, wherein devolatilization

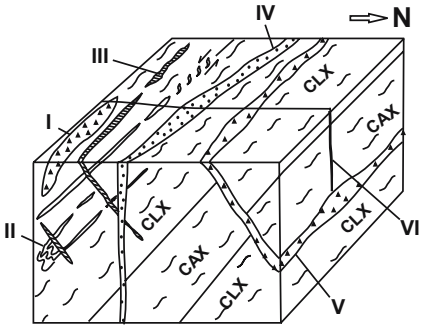

Fig. 3 Block diagram illustrating the mode of occurrence of the gold-mineralised vein types at the Fazenda Brasileiro deposit, according to (Mello et al. 1996)

reactions during the regional metamorphism and mantle–magmatic sources, contributed fluid components (Xavier 1991; Xavier et al. 1994).

Materials and methods

Sampling

Samples of the Teofilândia and Ambrósio domes and the Trilhado pluton were collected with the purpose of constraining the age of the felsic magmatism in the RIGB by SHRIMP U–Pb geochronology (Fig. 2). The Trilhado pluton, in the mid-north sector of the RIGB, is a small, elliptical, isotropic and undeformed body, previously interpreted as post-tectonic in relation to the RIGB evolution (Silva 1984). This pluton consists of a medium-grained leucocratic granodiorite composed of zoned plagioclase (50%), quartz (33%), K-feldspar (7%) and biotite (4%). Zircon and monazite crystals and opaque minerals occur as accessory minerals, whereas sericite and carbonate are secondary minerals derived from the alteration of plagioclase (5%).

The Teofilândia dome, in the southern portion of the RIGB, is a tonalite to granodiorite pluton with porphyritic texture and locally igneous bedding (Barrueto et al. 1998). Locally, the rocks exhibit features of heterogeneous deformation, indicated by the development of spaced cleavage planes and shear zones. The phenocrysts are plagioclase, less frequently K-feldspar and anhedral quartz crystals. The matrix contains plagioclase, quartz, amphibole, biotite, titanite and, as accessory minerals, clinozoisite, zircon and pyrite. In close association with the Teofilândia dome, there is also a quartz–feldspar porphyry that occurs in the southern sector of the greenstone belt, to the NE of the Fazenda Brasileiro deposit, in the Lagoa do Gato region (Barrueto et al. 1998; Nascimento et al. 1998; Gomes et al. 1998) (Fig. 2). The quartz–feldspar porphyry is composed of blue quartz and plagioclase phenocrysts immersed in a fine matrix containing mainly sericite, quartz and, subordinately, chlorite and pyrite.

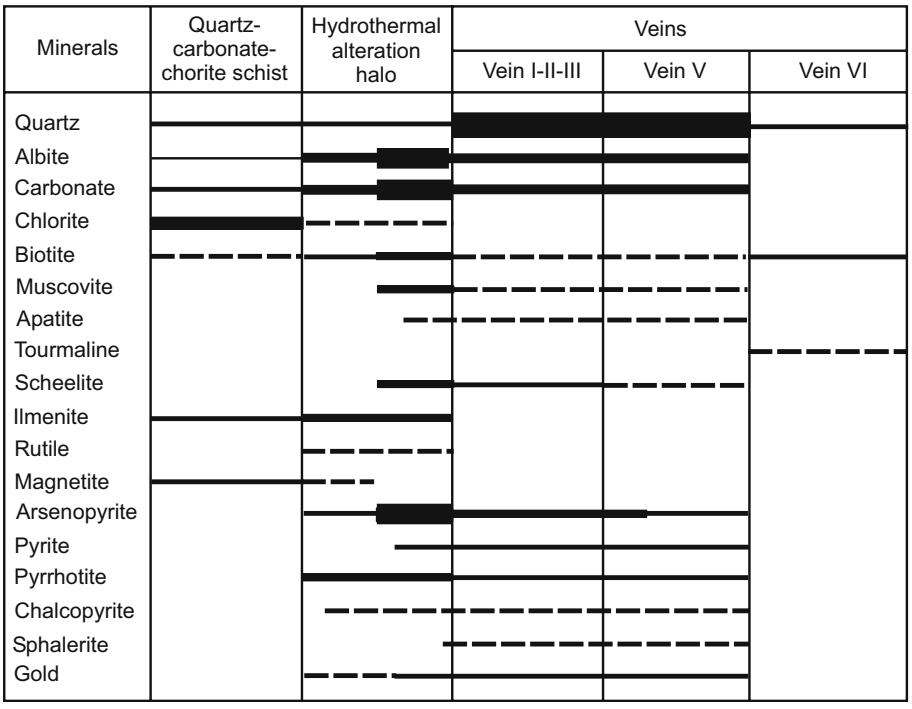

Fig. 4 Schematic evolution of the alteration and ore mineral assemblages at the *Fazenda Brasileiro* mine

The Ambrósio dome outcrops in the central sector of the greenstone belt where it delineates a 40 km by 4 km intrusion that occupies the core of an antiformal structure (Matos and Davison 1987). The central part of the dome is mainly dominated by a slightly deformed to massive or porphyritic granodiorite, with subordinate amounts of post-tectonic granite and pegmatite dykes and quartz veins. Enclaves of banded gneisses and migmatites, with strong mylonitic fabric, are found particularly concentrated along the margins of this dome (Lacerda and Oliveira 1997).

To constrain the age of the metamorphism in the RIGB, samples of quartzite and amphibolite from the Caldeirão belt were taken for SHRIMP U–Pb dating of detrital zircon crystals and Ar–Ar dating of hornblende concentrates, respectively. The former were collected in the vicinity of Monte Santo village, where they underlie or are in tectonic contact with the RIGB supracrustals, and the latter in the eastern edge of the Ambrósio dome, in contact with tholeiitic basalts (Fig. 2).

Samples of coarse-grained micas from the hydrothermal alteration zones around vein types II (biotite), III (muscovite) and V (muscovite) of the Fazenda Brasileiro deposit (Fig. 3), were selected for Ar–Ar dating, with the purpose of constraining the age of the gold mineralisation in the RIGB.

Sample preparation, analytical procedures and criteria for rejecting data

SHRIMP U–Pb ages Samples were crushed and pulverised in grain sizes between 250–150 mesh and 150–80 mesh. After nylon tissue sieving, the powders were washed and the resulting material subjected to heavy-liquid and magnetic separation techniques to concentrate the heavy minerals. Zircon, monazite and xenotime crystals were handpicked from the concentrate and mounted on epoxy resin with the following standards: CZ3 for zircons (Sri Lankan zircons with $^{206}Pb/^{238}U$=0.0914, corresponding to an age of 564 Ma; Pidgeon et al. 1994), MAD for monazite (514 Ma; Kinny 1997) and XTC for xenotime (2632 Ma; used in the Perth SHRIMP II Laboratory). Subsequently, back-scattering electron and charge contrast images (Griffin 1997a,b; Danilatos 1993) were obtained from all mounts on an environmental electron microscope together with photomicrographs to select appropriate crystals and areas for SHRIMP U–Pb analyses, in terms of size, growth morphology and internal structure.

The analytical procedures for zircon and the general operating conditions adopted in the SHRIMP are described by Compston et al. (1984), Nelson (1997) and Smith et al. (1998). Specific analytical routines were used for monazite (Kinny 1997) and xenotime (McNaughton et al. 1999). The corrections for common lead were made assuming the composition of common lead from Broken Hill for all the unknown analyses, except for xenotime samples (9905-D), where the (Cumming and Richards 1975) lead composition was used. In the data assessment, the $^{207}Pb/^{206}Pb$ ages were used, which are considered more reliable for ages with concordant data over 800 Ma, whereas the $^{206}Pb/^{238}U$ ages are preferred for ages less than 800 Ma.

The data considered acceptable and used for the calculation of the age averages fulfil the following requisites: (1) analyses are considered acceptable if they lie within 5% of concordia (i.e. 95 and 105% concordant); (2) results with less than 2% of ^{206}Pb, attributed to the correction of common lead; and (3) good alignment between the more discordant data and those concordant or close to the

concordia curve. Mixed ages, resulting from analyses of areas that included both core and rim were discarded. At the Perth SHRIMP II Laboratory, the analytical data are routinely processed utilizing the Krill data reduction programme, and later plotted in the Wetherill (1956) concordia diagram by means of the Plonk programme. The individual analyses were plotted with 1σ errors, and the final age, calculated from a group of individual ages, was expressed with 2σ error.

Ar–Ar ages For the separation of amphibole, muscovite and biotite crystals, the samples were crushed, sieved between 60 and 100 mesh and washed for removal of the fine fraction. Subsequently, 99% pure concentrates were obtained by using heavy liquids, a Frantz electromagnetic separator and binocular microscope. The purification of the sample was rigorously performed under binocular microscope, by removal of composite grains and interferent minerals in the Ar–Ar analyses. The principal interferent minerals eliminated by manual picking were fuchsite (sample FB2G) and chlorite (samples FB11D). Other minor residues, including small quartz crystals, were also eliminated.

The Ar–Ar ages were obtained by the technique of fusion in stages using some milligrams of concentrate. The analytical procedures adopted during the $^{40}Ar/^{39}Ar$ analyses of the concentrates, the criteria and constants used in the processing of the data and in the calculation of the ages, follow those described by Snee et al. (1988).

Results of SHRIMP U–Pb dating

Felsic intrusives

Trilhado granodiorite Twenty-four analyses were obtained on 21 elongated, euhedral to subhedral, generally zoned zircon crystals from the Trilhado granodiorite (Sample 9857b). Most of the analyses were conducted on the rims and only six were obtained on the core of the investigated zircon crystals. The ages were quoted for grains with concordance between 93 and 105%. The analytical results are presented in Table 2 (see electronic supplementary material) and the ages plotted in the concordia diagram of Fig. 5. Seven analyses obtained from both the core and the rim of zircon crystals 7.1, 14.1, 15.1, 17.1, 24.2, 26.1 and 32.1 yield an average $^{207}Pb/^{206}Pb$ age of 2,155±9 Ma (Fig. 5), interpreted as the age of crystallisation of the granodiorite. Analyses 33.1 and 36.1 are reversely discordant and yielded significantly older $^{207}Pb/^{206}Pb$ ages, probably due to their high common Pb content (Table 2 in electronic supplementary material). The other analyses indicated varying degrees of discordance, related to the loss of radiogenic Pb.

Additional 13 U–Pb analyses were also conducted on monazite crystals taken from the same concentrate where the zircon crystals were selected (Table 3 in electronic supplementary material). The monazite U–Pb analyses are concordant (97–103%) and give an average $^{207}Pb/^{206}Pb$ age of 2,152±6 Ma (Fig. 5). This result is in good

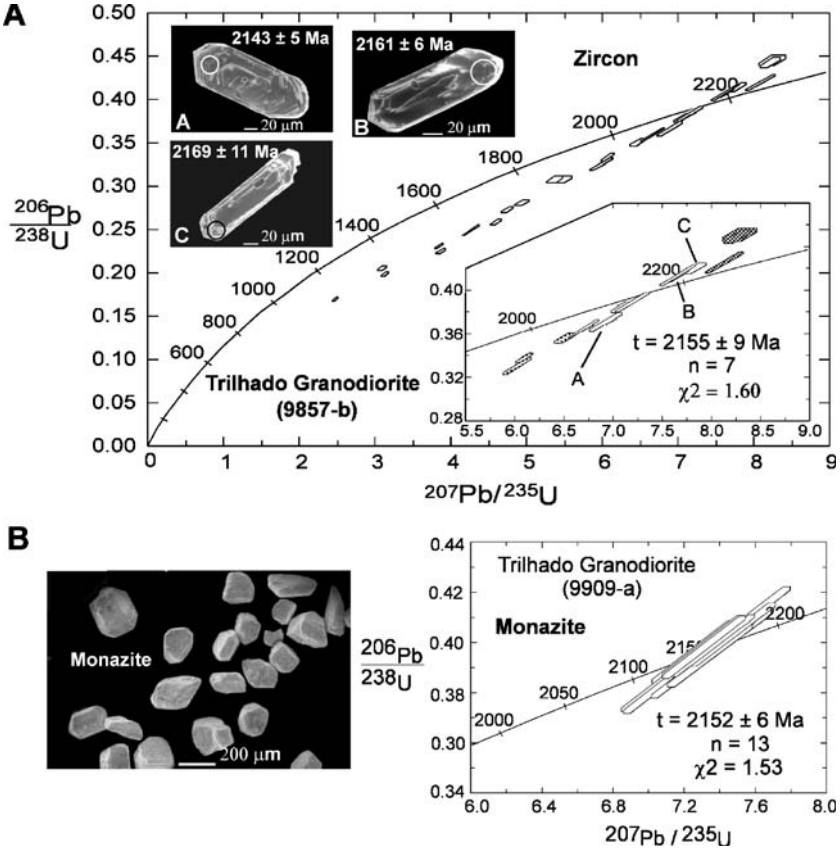

Fig. 5 Concordia plot showing CCI zircon and BSE monazite images from the *Trilhado* granodiorite (9857b). *Stippled error boxes* are rejected data. Twelve analyses of the CZ3 standard indicated a U/Pb calibration error of 1.28%. Seven analyses in the MAD standards indicated a U/Pb calibration error of 3.09%

agreement with the zircon data and together may be interpreted as the crystallisation age of the Trilhado granodiorite.

Teofilândia tonalite The zircon crystals selected for the SHRIMP U–Pb analyses of the Teofilândia tonalite (sample 9857a) consist of a single morphological type. They comprise euhedral crystals with colours varying from light yellow to brownish yellow, which frequently display oscillatory magmatic zoning (Fig. 6). Twenty-one analyses were performed on these zircon crystals (Table 4 in electronic supplementary material). Ten analyses on zircon (1.1, 6.1, 7.1, 9.1, 12.1, 26.2, 32.2, 33.2, 34.1 and 53.1) produce an average $^{207}Pb/^{206}Pb$ crystallisation age of 2,130±7 Ma.

Quartz–feldspar-porphyry The zircon crystals from the quartz–feldspar porphyry selected for U–Pb SHRIMP analyses are similar to those obtained in the Teofilândia tonalite (Fig. 7). A total of 22 analyses were obtained on 21 zoned magmatic zircons (Sample 9857c) (Table 5 in electronic supplementary material). From these, five analyses (12.1, 23.1, 25.1 32.1, and 36.1) of five zircon crystals produced a concordant $^{207}Pb/^{206}Pb$ crystallization age of 2,128±8 Ma (Fig. 7).

Ambrósio dome Samples of massive and porphyritic granodiorite, granite dyke and a gneiss enclave within the massive granodiorite were selected in the Ambrósio dome for the SHRIMP U–Pb age determinations.

Zircon crystals from the massive granodiorite (Sample 9906a) exhibit poorly developed prismatic faces and are weakly zoned. They are subhedral and all exhibit sub-rounded to rounded terminations. Most of the crystals are turbid and dark brown in colour, probably due to metamictisation (Fig. 8).

Four groups of $^{207}Pb/^{206}Pb$ ages were defined in 27 analyses of 23 zircon crystals (Table 6 in electronic supplementary material; Fig. 8):

- Group 1: Average $^{207}Pb/^{206}Pb$ age of 2,077±22 Ma (analyses 17.1, 24.1, 24.2 and 50.1). Although they form a distinct group, their Th/U ratios are variable on the basis of the good concordance indicating values typical of igneous zircons (higher Th/U ratio) for the analyses 24.1 and 24.2, and typical of metamorphism (lower Th/U ratio) (Willians and Claesson 1987; Willians 1992; Pidgeon 1992; Kinny and Nutman 1996; Seth et al. 1998; Åhäll et al. 1998) for analyses 17.1 and 50.1. These two latter analyses were performed on clean crystals with rounded outlines indicating corrosion, a typical feature related to metamorphism. It is possible that these features reflect the syntectonic nature of the Ambrósio dome
- Group 2: Average $^{207}Pb/^{206}Pb$ age of 2,937±16 Ma (analyses 1.1, 9.1, 25.1, 29.1, 32.1, 43.1, 43.2 and 44.1)
- Group 3: Average $^{207}Pb/^{206}Pb$ age of 3,111±13 Ma (analyses 4.1 and 47.1)
- Group 4: Average $^{207}Pb/^{206}Pb$ age of 3,162±13 Ma (analyses 3.1, 28.1, 33.1 and 34.1)

The wide scatter of the analyses precludes a clear definition of a group of ages representative of the crystallisation age of the massive granodiorite, but the younger group of 2,077±22 Ma may mark the emplacement age of this rock, despite the great imprecision of the data. The older ages are interpreted to represent inherited crystals.

The zircon crystals from the porphyritic granodiorite (Sample 9906c) are mostly long euhedral to subhedral prisms and commonly exhibit sub-rounded to rounded pyramidal terminations. More subordinately, they show fine overgrowths enveloping an euhedral core or exhibit oscillatory

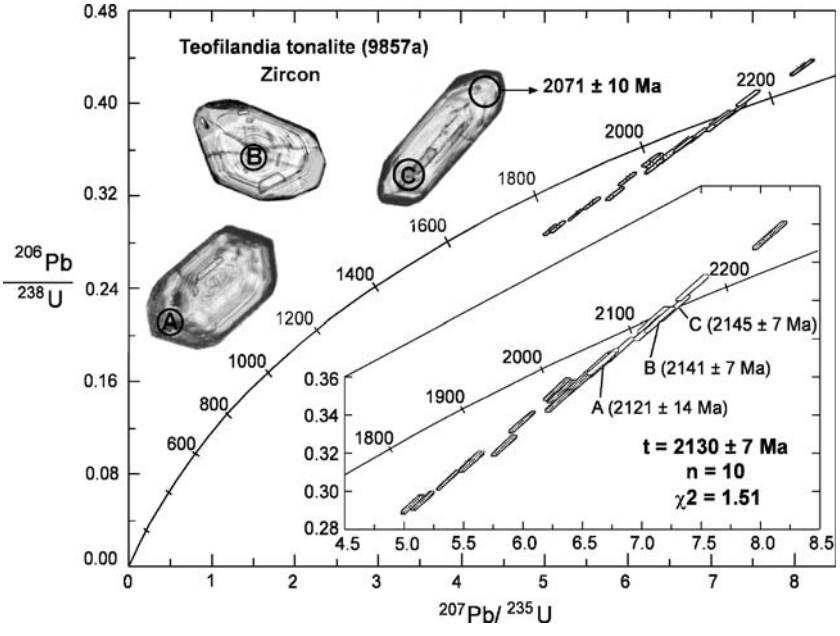

Fig. 6 $^{207}Pb/^{206}Pb$ SHRIMP ages of zircons from the *Teofilândia* tonalite (9857a). *Stippled error boxes* are rejected data. Photomicrographs of representative zircons: **a** 140×60 μm, **b** 107×51 μm, **c** 123×42 μm. Ten analyses on the CZ3 standard indicate an U/Pb calibration error of 1.72%

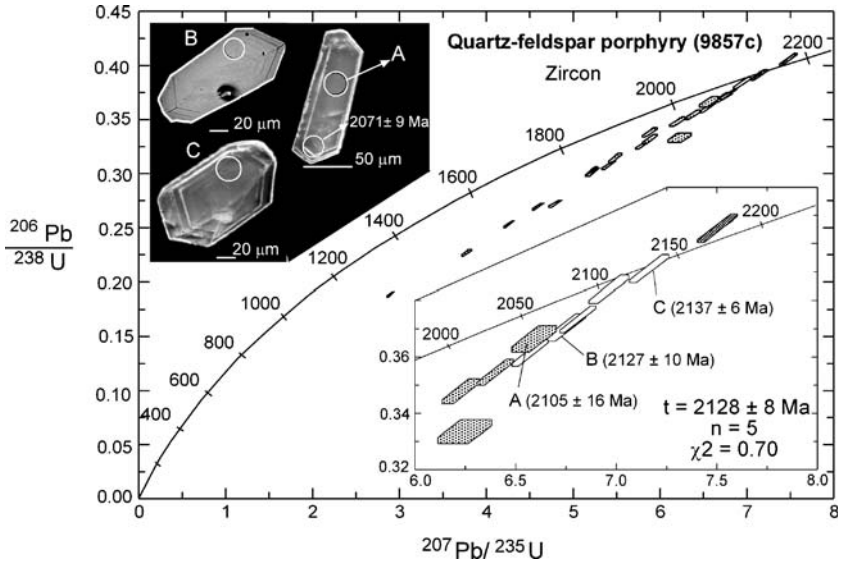

Fig. 7 $^{207}Pb/^{206}Pb$ SHRIMP ages of zircons from the *Teofilândia* quartz-feldspar porphyry (9857c). *Stippled error boxes* are rejected data. Spot locations of the analyses are shown in **a** BSE and **b**, **c** CCI images of zircons. Ten analyses performed on the CZ3 standard indicate a U/Pb calibration uncertainty of 1.28%

zoning reflecting the pyramidal shape of the grain. They display yellow to light yellow, brownish yellow and brown colours. Most of the analyses were performed on areas of the cleanest crystals in regions without zoning (Fig. 9). From a total of 11 analyses (Table 7 in electronic supplementary material), analyses 21.1, 48.1 and 56.1 form a group with an average $^{207}Pb/^{206}Pb$ age of 2,063± 55 Ma (Fig. 9).

The analyses 35.1, 38.1 and 34.1 also show a good alignment with ca 2,063 Ma analyses, but were excluded from the age calculation due to the high degree of discordance. As with the massive granodiorite, the younger ages may define the crystallisation age of the porphyritic granodiorite, and the older ages may represent inherited zircons.

Scarce zircon crystals, in general with strong metamictisation, were observed in samples from the granite dyke. For this reason, they were considered unsuitable for analyses and xenotime crystals (Sample 9905d) were selected instead for analyses. Xenotime appears as coarse euhedral crystals and exhibits magmatic zoning (Fig. 10). An average $^{207}Pb/^{206}Pb$ age of 2,080±2 Ma obtained from 16 analyses of 15 xenotime crystals is interpreted as the crystallisation age of the granite dyke (Table 8 in electronic supplementary material; Fig. 10).

The zircon crystals separated from the gneiss enclave (Sample 9906b), hosted by the massive granodiorite, include long and short prisms. The crystals generally exhibit sub-rounded to rounded terminations and narrow zoned rims enveloping euhedral to subhedral cores. They are brown to dark brown coloured, with a few exhibiting light yellow and, rarely, colourless (Fig. 11). Some zircon crystals display ghosts of the original zoning, indicating partial recrystallisation of these areas.

Two distinct average $^{207}Pb/^{206}Pb$ ages were grouped from seven analyses conducted on seven light yellow zircon crystals (Table 9 in electronic supplementary material;

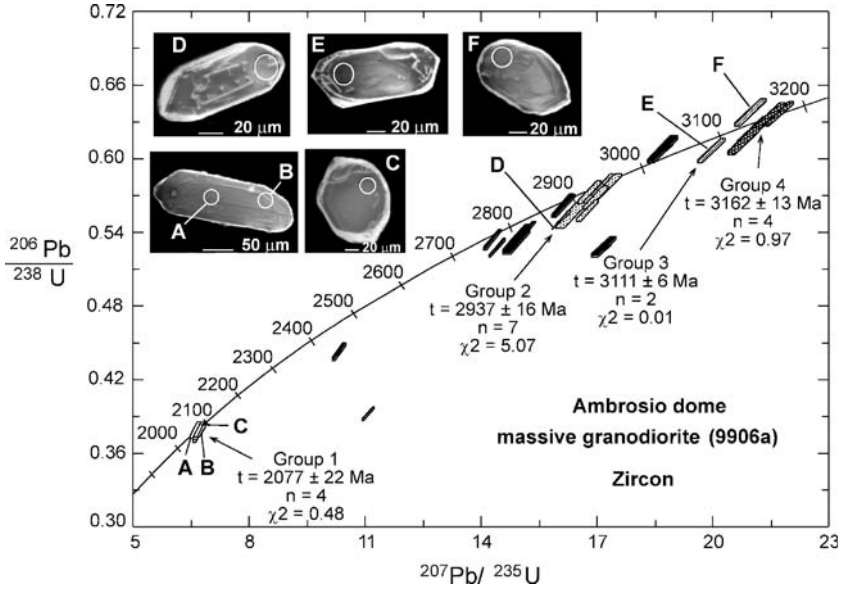

Fig. 8 $^{207}Pb/^{206}Pb$ SHRIMP ages of zircons from the massive granodiorite (9906a) of the *Ambrósio* dome. Representative CCI zircon images are indicated on the concordia with spot location. Thirteen analyses in the CZ3 standard indicated a U/Pb calibration error of 1.48%

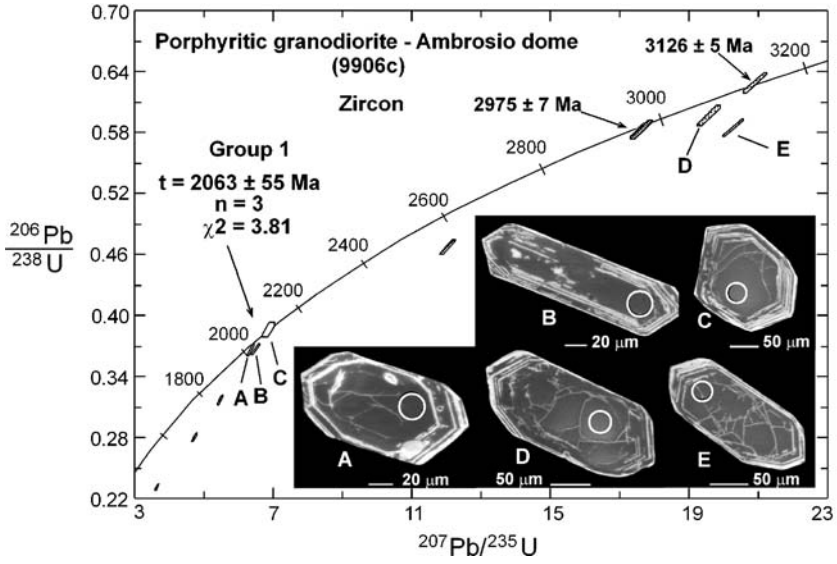

Fig. 9 $^{207}Pb/^{206}Pb$ SHRIMP ages of zircons from the porphyritic granodiorite (9906c) of the *Ambrósio* dome. Representative CCI zircon images are indicated on the concordia with spot location. Thirteen analyses in the CZ3 standard, indicated a U/Pb calibration error of 1.48%

Fig. 11): 3,094±21 Ma (analyses 12.1, 14.1 and 35.1) and 3,159±18 Ma (analyses 13.1, 18.1 and 40.1). These ages are interpreted as ages of the igneous precursors of the gneiss. Only analysis 39.1 was discarded, for not aligning with either of the two groups, possibly because of loss of radiogenic Pb similar to the analyses of group 2.

Caldeirão Belt quartzite

Zircon crystals (sample 98102c) from the Caldeirão Belt quartzite have a great variety of external and internal morphological aspects. Most are euhedral to subhedral prismatic crystals, with sub-rounded terminations and range in colour from light yellow to yellow, red, or are colourless. Some are multi-faceted showing bi-pyramidal terminations, whereas a few are round typical of a detrital origin. Most of the internal features are characterised by a faint and zoned core, frequently cracked, rimmed by thin overgrowths, suggesting recrystallisation accompanied by newer zircon growth (Pidgeon 1992; Pidgeon and Wilde 1998).

Fifty-one spots were analysed from 39 zircon crystals from the quartzite, from which the following age groups could be distinguished (Table 10 in electronic supplementary material; Fig. 12):

The overgrowth zones yielded an average $^{207}Pb/^{206}Pb$ age of 2,076±10 Ma (analyses 5.1, 14.1, 26.1, 43.1, 61.1, 62.1 and 63.1; group 1), on zircon crystals with low Th/U ratios (<0.1), with the exception of analysis 61.1 (ratio of 0.159), typical of metamorphic zircons (Willians and

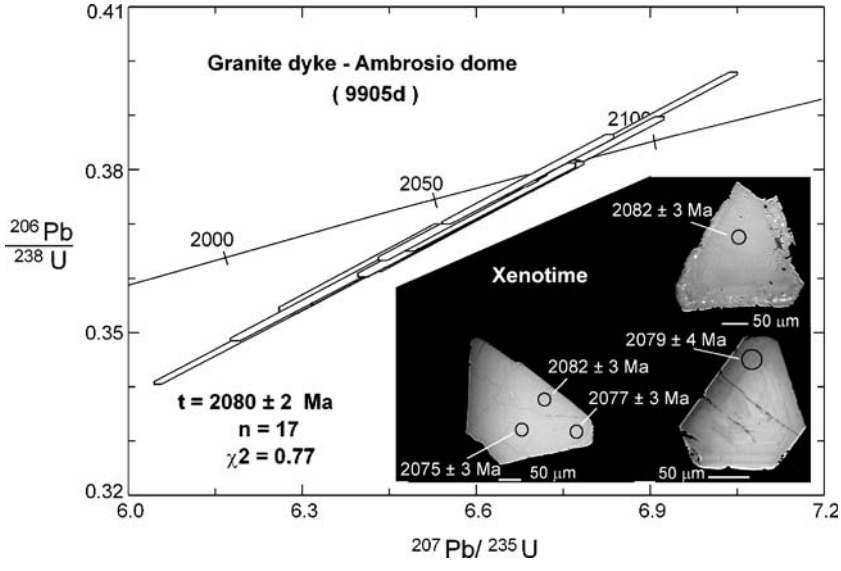

Fig. 10 $^{207}Pb/^{206}Pb$ SHRIMP ages of xenotime from granite dyke sample (9905d) of the *Ambrósio* dome. Xenotime BSE image shows the spot location of the analysis. Eight analyses in the XTC standard indicated a U/Pb calibration error of 2.18%

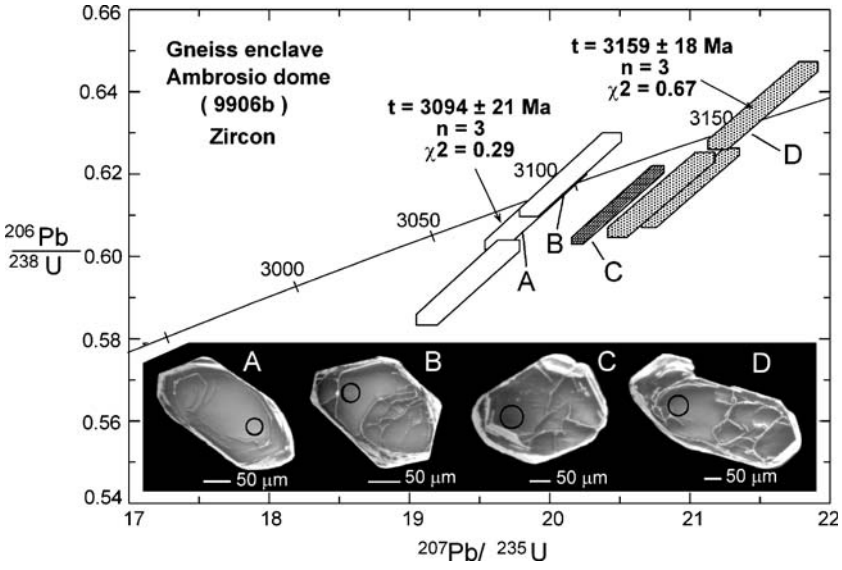

Fig. 11 $^{207}Pb/^{206}Pb$ SHRIMP ages of zircons from the gneiss enclave in *Ambrósio* dome granodiorite (9906b). Representative CCI zircon images are indicated on the concordia with spot location. Thirteen analyses obtained in the CZ3 standard indicated a U/Pb calibration error of 1.48%

Claesson 1987; Pidgeon 1992; Kinny and Nutman 1996) (Fig. 12). This Palaeoproterozoic age was attributed to the Trans-Amazonian metamorphism that affected the quartzite and the RIGB.

Archaean $^{207}Pb/^{206}Pb$ ages, yielded from zircon cores, of 3,051±13 Ma (group 2), 3,097±11 Ma (group 3) and 3,204±9 Ma (group 4) were considered as the crystallisation ages of the distinct source rocks for the quartzite. One single analysis (51.1) provided a concordant $^{207}Pb/^{206}Pb$ age of 2,687±16 Ma (1σ), interpreted as the possible maximum age of sedimentation.

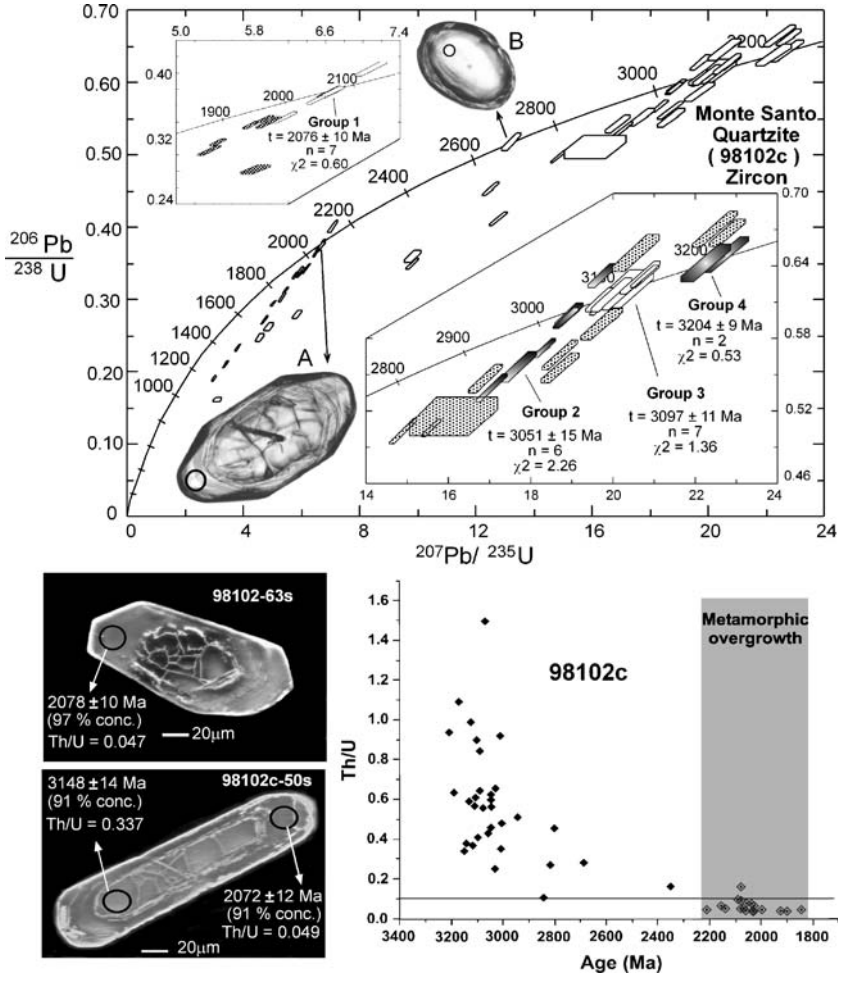

Fig. 12 $^{207}Pb/^{206}Pb$ SHRIMP ages of detrital zircons from the *Monte Santo* quartzite (98102c), *Caldeirão* Belt, with photomicrographs indicating the spots of the analyses and Th-U diagram. *Stippled error boxes* are discarded analyses. *Empty* and *shaded boxes* are considered for age analyses. Eight analyses obtained in the CZ3 standard, indicated a U/Pb calibration error of 2.17% for this sample

Results of Ar–Ar dating

Amphibolite (MPANF2D and MPANF3)

Hornblende concentrates from the amphibolite samples MPANF2D and MPANF3 were heated in 14 and 12 steps, respectively (Table 11 in electronic supplementary material; Fig. 13). The analysis of the spectrum of sample MPANF2D indicates that the initial steps of low temperature heating (9.1% of the spectrum) register a wide variation in the ages, with accentuated retrogressions in the temperature range of 750 to 1000°C. The stabilisation occurs at higher temperatures with 91% of ^{39}Ar released, defining a plateau age with six steps, indicating an age of 2,080±5 Ma. In the spectrum of sample MPANF3, the high ages obtained in the first 1.1% of the spectrum, decrease to 2,132 Ma and 2,134 Ma in the lower temperature steps (3.1% of ^{39}Ar released). This is followed by a new ascension and regression up to 2,124 Ma (with 43.4% of ^{39}Ar released). From this point, the spectrum of ages tends to stabilise, indicating small disturbances in 2,084 Ma and 2096 Ma (60.4% of ^{39}Ar released). The final steps of the spectrum define a plateau segment with an average age of 2,128±4 Ma, comprising 39.6% of gas released in three steps.

The age spectra of the two samples indicate small differences in the first stages of extraction and a tendency towards stabilisation in the following stages, more effective in the sample MPANF2, located further away from the Ambrósio dome. Sample MPANF3, closer to the contact with the Ambrósio dome yielded an older age. The isochrons obtained in ^{40}Ar/^{36}Ar vs ^{39}Ar/^{36}Ar diagrams indicate an age of 2,080±5 Ma (2σ, *n*=5) for sample MPANF2D and 2,108±5 Ma (2σ, *n*=8) for sample MPANF3. In the former, the isochron age is the same age as that of the plateau, whereas the latter yielded an age correction to 2,108±5 Ma (2σ, *n*=8).

The age of 2,080±5 Ma obtained in the samples MPANF2D is in agreement with the SHRIMP U–Pb age of emplacement of the Ambrósio dome of 2,080±2 Ma and may therefore reflect the amphibolite facies metamorphism at the edges of the pluton. The 2,108±5-Ma isochron age (MPANF3) can be attributed either to: (1) the presence of remaining ^{40}Ar related to heating previous to the emplacement of the Ambrósio dome; and (2) ^{40}Ar introduced into the amphiboles due to the proximity of the amphibolite with the granodiorite, resulting from intrusion-related deformation that caused migration and interaction of fluids between the granodiorite and amphibolite (cf. Harrison and McDougall 1985; Cumbest et al. 1994). The inherited

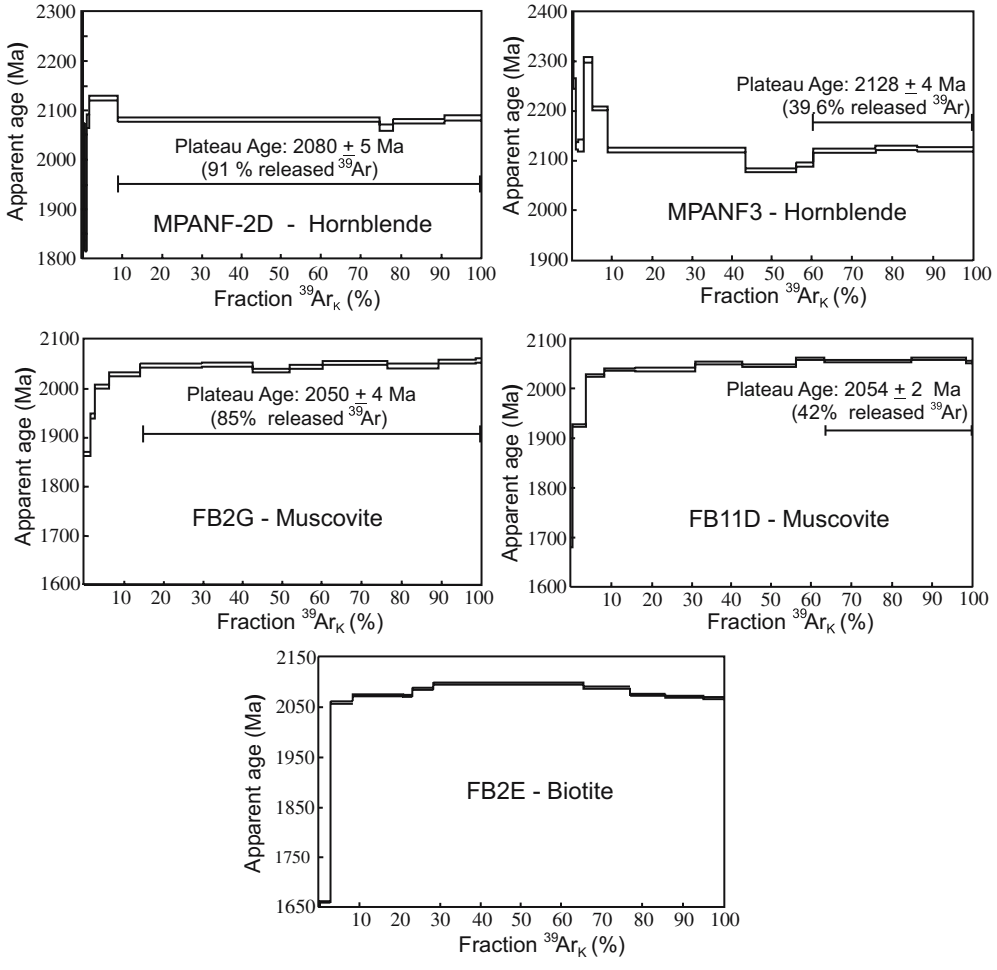

Fig. 13 Spectra of ^{39}Ar/^{40}Ar age in hornblende from amphibolites MPANF2d and MPANF3, hydrothermal muscovite from veins III (FB2G), V (FB11D), and biotite from vein II (FB2E), all of the Fazenda Brasileiro gold deposit

argon may have been introduced during heating related to the magmatism between 2,152 and 2,130 Ma or to the ca 2,100 Ma felsic intrusions. Regardless of the exact mechanism, the presence of excess argon renders the MPANF3 "age" invalid.

Vein alteration muscovite (FB2G and FB11D) and biotite (FB2E): Fazenda Brasileiro gold deposit

Muscovite samples at hydrothermal alteration zones vein III (FB2G) and vein V (FB11D) were heated in 12 stages and the analytical results are presented in Table 11 (see electronic supplementary material) and Fig. 13. The spectrum of sample FB2G ascends uniformly in the first four steps of heating (14.1% of ^{39}Ar released) and defines a plateau of 2050±4 Ma, with eight steps representing 85.8% of ^{39}Ar released. The age spectrum of sample FB11D indicates some loss of argon in the first 0.1% of the spectrum, but evolves to an age close to the plateau at higher temperatures, defining a plateau segment at 2,054±2 Ma, with three heating steps with 42% of ^{39}Ar. Both ages are rigorously concordant and reflect the age at which the Ar–Ar system closed for the hydrothermal muscovite, therefore, marking the minimum age for the gold mineralisation.

The biotite samples from the vein II alteration zone (FB2E) were heated in 12 stages (Table 11 in electronic supplementary material). These samples provided disturbed spectra, possibly related to intergrowths of chlorite in the biotite, with humps of higher ages in the central parts (Fig. 13). These humps may be related to greater Ca contents or indicate small excesses of Ar (Plint and McDonough 1995). The spectrum of sample FB2 indicates an apparent age between 2,040 and 2,065 Ma, excluding the first and last lower ages. This age interval is consistent with the 2,050±4 Ma muscovite age.

Discussion

Age of the RIGB basement and the felsic intrusions

The SHRIMP U–Pb results indicate the existence of an extensive segment of the Archaean continental crust, with diverse components between 2,937 Ma and 3,204 Ma, which acted as the basement for the rocks of the RIGB. This is consistent with the abundant presence of inherited zircons in the massive granodiorite of the Ambrósio dome, defining age groups of 2,937±16 Ma, 3,111±13 Ma and 3,162±13 Ma, and in the gneiss enclave in the same dome with average ages of 3094±21 and 3159±18 Ma. This inheritance suggests an important phase of crustal reworking, during the most significant tectono-thermal event between 2,130 and 2,080 Ma, which produced the abundant syncollisional felsic plutonism in the region. Similar ages were obtained for the Caldeirão Belt quartzite zircons at 2,943±7 Ma, 3,051±13 Ma, 3,097±11 Ma and 3,204±9 Ma.

The SHRIMP U–Pb data obtained in zircon, monazite and xenotime crystals indicate ages from 2,155 Ma to 2,080 Ma for the felsic intrusives investigated in the RIGB. The zircon crystals from the Trilhado granodiorite (sample 9857b) indicate a ^{207}Pb/^{206}Pb crystallisation age of 2,155±9 Ma. This age is consistent with the ^{207}Pb/^{206}Pb age obtained in monazites (sample 9909a) that provide a more precise crystallisation age of 2,152±6 Ma. Together, these ages mark the onset of felsic magmatism in the RIGB, indicating that the Trilhado granodiorite was emplaced before the syntectonic intrusions of the RIGB. The zircon crystals from the Teofilândia tonalite and quartz–feldspar porphyry constitute the same morphological type. The ^{207}Pb/^{206}Pb ages obtained for these rocks yielded averages of 2,130±7 Ma and 2,128±8 Ma, respectively, indicating that they are cogenetic and temporally related to the Barrocas granodiorite, previously dated at 2127±5 Ma (Alves da Silva 1994).

In the Ambrósio dome, a wide variation of ages in groups of morphologically distinct zircons was obtained. The large number of metamictic and inherited zircon crystals did not allow precise definition of the crystallisation age for the massive (9906a) and porphyritic (9906c) granodiorite samples. In the former, four concordant analyses define a ^{207}Pb/^{206}Pb age of 2,077±22 Ma, whereas in the latter three analyses define a ^{207}Pb/^{206}Pb age of 2,063±55 Ma. Most of the analyses in the massive granodiorite constrain the age of inheritance, with ^{207}Pb/^{206}Pb ages of 2,937±16 Ma, 3,111±13 Ma and 3,162±13 Ma. These ages either relate to igneous rocks within the basement or are derived from metasedimentary lithologies in the basement rocks with a maximum age of 2,937±16 Ma. This is corroborated by the analyses in seven zircon crystals from the gneiss enclave, which indicate two groups of ages (3,094±21 Ma and 3,159±18 Ma).

The time of emplacement of the Ambrósio dome is constrained by the xenotime age from the granite dyke at 2,080±2 Ma, interpreted as the crystallisation age of this rock. The xenotime presents a less disturbed U–Pb system, although normally it contains higher uranium concentrations than the coexisting zircons (Aleinikoff and Graugh 1990; Eliasson and Schöberg 1991). The presence of this mineral points to a greater differentiation of the rock, indicating a late magmatic phase (Eliasson and Schöberg 1991). The blocking temperature of this mineral is currently poorly established, but is at least >650°C (Heaman and Parrish 1991), with some temperature estimates as high as 700–750°C (similar to that of monazite; Aleinikoff and Grauch 1990), and >800°C (Kamber et al. 1998).

The xenotime data from the felsic dyke are consistent with the interpretation of the younger ages, obtained in the zircon crystals from the granodiorites, as the crystallisation ages of these rocks. Therefore, 2,080±2 Ma is considered the emplacement age of the Ambrósio dome and marks the final stages of the granite formation in the RIGB. This time coincides with the period of significant heating in the RIGB, marked by the U–Pb ages in the detrital zircons from the

Caldeirão Belt quartzite and Ar–Ar in hornblende. These data and the ages provided by various other syncollisional granitoids, suggest a period of great orogenic activity between 2,100 and 2,080 Ma.

Age of the peak of metamorphism

The age of 2076±10 Ma obtained on the overgrown rims of the detrital zircons from the Caldeirão Belt quartzite (98102-c) was interpreted as the age of the metamorphic peak of the RIGB. This interpretation is based on the following considerations: (1) the data were obtained on overgrown areas (restored crystals) of detrital zircons (Pidgeon 1992; Pidgeon and Wilde 1998), (2) in these areas low Th/U ratios typical for metamorphic zircons were obtained (Willians and Claesson 1987; Pidgeon 1992; Kinny and Nutman 1996) and (3) the blocking temperature of metamorphic zircons of around 600°C (Heaman and Parrish 1991).

The ages of 3,051±13, 3,097±11 and 3,204±9 Ma, obtained in the internal regions of the zircon crystals, probably reflect the source areas for the sediments. The data provided by the detrital zircons from the Caldeirão Belt quartzite are of great significance in the understanding of the RIGB crustal history. They mark, with a high degree of reliability, the age of the principal tectono-thermal event that affected the RIGB, and reveal the same Archaean components identified by the zircons inherited of the Ambrósio dome. Additionally, the quartzite may have been one of the components of the RIGB basement, considering the age of 2,937±16 Ma as the maximum age of sedimentation.

The maximum age of sediment deposition is certainly older than this metamorphic event but younger than the youngest detrital zircon found, with the concordant single age of 2,687±16 Ma (Mello et al. 1999; Oliveira et al. 2002).

The concentrates of hornblende obtained in the samples from amphibolites close to the Ambrósio dome indicate distinct ages, which may correspond to a period of greater heating in the RIGB. The youngest Ar–Ar age of 2,080±5 Ma probably indicates the emplacement of the Ambrósio dome. This age is rigorously concordant with the metamorphic age provided by the detrital zircons and may therefore correspond to the amphibolite facies metamorphism at the contact of the Ambrósio dome with the supracrustal rocks. The syncollisional granite formation must have reached its thermal peak around 2,076±10 Ma.

Timing of gold mineralisation

The $^{40}Ar/^{39}Ar$ data obtained for hydrothermal muscovites from vein III (FB2G) and vein V (FB11D) of the Fazenda Brasileiro deposit gave similar ages of 2,050±4 Ma and 2,054±2 Ma, respectively, These values are interpreted as the minimum ages for the gold mineralisation at the Fazenda Brasileiro deposit. The thermal history related to a mineralising event at Fazenda Brasileiro indicates that the hydrothermal muscovite must have crystallised quite close to the argon retention temperature. The P–T estimates for the mineralising fluids at the Fazenda Brasileiro mine are 400–500°C and 1.8–3.5 kbar (Xavier et al. 1994), near the temperature of retention for argon in muscovite (350±50°C; McDougall and Harrison 1988). This suggests that the Ar–Ar age of the mineralisation must be close to the true age of gold deposition. On this basis, it is considered that the mineralisation must have occurred at least 50 Ma after the orogenesis responsible for the closure of the RIGB basin.

Alternatively, the possibility must be considered of occurrence of the mineralisation in various episodes; in this case, the Ar–Ar system would be registering only the last episode.

Conclusions

The evolution of the RIGB must have occurred in two stages, succeeding mafic volcanism: the older stage, within the 2,152–2,130 Ma interval, is characterised by the addition of magmas to the pre-existing Archaean continental crust (2,937–3,162 Ma) and the youngest, between 2,130 and 2,080 Ma, by a period of great tectonic and thermal activity, responsible for the syntectonic granitoids produced by crustal reworking, during the closure of the back-arc basin (Fig. 14).

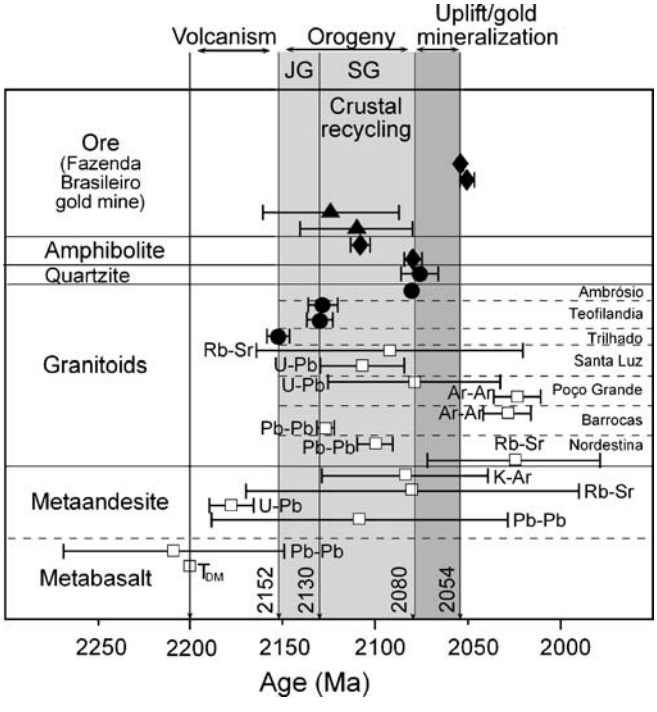

Fig. 14 Crustal evolution and gold mineralisation in the Rio Itapicuru greenstone belt. The *solid black symbols* correspond to the data obtained in this work (*circle* U–Pb SHRIMP ages, *rhombus* Ar–Ar ages, *triangle* K–Ar ages). The *empty squares* correspond to data obtained from the references (see Table 1). *JG* Juvenile granitoids, *SG* Syntectonic granitoids

The older stage is marked by the emplacement of the Trilhado granodiorite and the Teofilândia tonalite, respectively, at 2,152±6 Ma and 2,130±7 Ma. This period of ca 22 Ma was possibly contemporaneous with D1 deformation and the formation of the volcanic centres (andesitic lavas and subvolcanic rocks) of the magmatic arc. This scenario is consistent with the evolutive model in which the subduction of the oceanic crust under the continental block (ca 2200–2152 Ma) was responsible for the generation of synvolcanic granodiorite-tonalites (2152–2130 Ma).

The closure of the back-arc basin must have occurred in the period ca 2,130–2080 Ma, thus marking the second stage of crustal evolution (event D2). In this period, great volumes of syntectonic felsic intrusives were generated, related to the most important thermal event that affected the rocks and isotopic systems of the orogen. The syntectonic characteristics of the Ambrósio dome and the indications of crustal contamination, attributed to the innumerable enclaves of gneissic–migmatitic rocks, are reported by Matos and Davison (1987), Alves da Silva (1994) and Lacerda and Oliveira (1997). These are further supported by the abundance of zircon crystals inherited in the massive and porphyritic granodiorite samples of the Ambrósio dome, which suggest reworking of the Archaean rocks. The age determination of these rocks was hindered by the predominance of inherited zircons, with groups of ages between 2,937 and 3,162 Ma. The Archaean inheritance and the ages of 3,094±21 Ma and 3,159±18 Ma obtained in the gneiss enclave in the Ambrósio dome, indicate basement components with ages between 2,937 and 3,162 Ma.

As the granite dykes and pegmatites of the Ambrósio dome must represent a late stage of the synorogenetic magmatism, the crystallisation age of 2,080±2 Ma obtained in xenotime may be interpreted as the minimum crystallisation age for this dome, marking the end of the plutonic activity in the orogen.

The geological and geochronological data indicate that the peak of the tectono–metamorphic–magmatic activity must have occurred during the collisional period between 2,130 and 2,080 Ma. The Transamazonian thermal event is apparent in the Rb–Sr, K–Ar and Pb–Pb data of the granitoid rocks and felsic volcanics, with signs of rehomogenisation at ca 2,100 Ma. In the Caldeirão Belt quartzite the Transamazonian thermal effects in the U–Pb system are preserved in the metamorphic overgrowths of the detrital zircons at 2,076±10 Ma. This age is within error of the Ar–Ar age of 2,080±5 Ma obtained in hornblendes (sample MPANF2) at the edge of the Ambrósio dome, and with the age of 2,080±2 Ma obtained in xenotime (granite dyke in the Ambrósio dome) that determines the age of emplacement of this dome. The set of geochronological data indicates that the syn-D2 metamorphism must have reached maximum intensity between 2,100 and 2,080 Ma, locally with temperatures in the amphibolite facies, indicated by the mineral paragenesis and by the blocking temperatures of the metamorphic zircons and hornblende, respectively, around 600°C and 530±40°C (Heaman and Parrish 1991).

As the spectra of Ar–Ar ages in hydrothermal muscovites did not reveal disturbances, they are interpreted here as the crystallisation ages of this mineral. The age of 2,050±4 Ma, represented by the greater quantity of gas released, is the best estimate of the age of the mineralisation. This age is concordant with the interval of ages between 2,040 and 2,065 Ma, indicated by the hydrothermal biotite of vein II. These values are also concordant with the lower limit of the interval of ages between 2,050 Ma and 2,073 Ma, obtained in the biotite samples from the metabasalt enclave in the tonalite. The latter must mark the resetting of the Ar–Ar system after 2,130 Ma (the tonalite age) and, therefore, may indicate the cooling of the syntectonic granitoids (of the Ambrósio type) and/or the hydrothermal activity of the mineralising fluids.

The mineralisation must have occurred ca 30 million years after the peak of the metamorphism, in response to the pressure relief in the rocks during uplift and exhumation of deeper crustal levels. On the other hand, diachronism of the mineralisation may be argued, if one considers the possibility of the occurrence of episodic pulses. In this case, the mineralisation may have occurred in a period of ca 30 million years, between 2080 and 2050 Ma.

In general, the geochronological data in the RIGB do not show superimposition of events after the collisional period (2,152–2,080 Ma) (Fig. 14), so that the $^{40}Ar/^{39}Ar$ ages registered in the minerals of low retentivity, must record the period of regional cooling and the hydrothermal mineralising event of low temperature, relating to the uplift and exhumation of the orogen, where the RIGB is situated.

The gold mineralisation in the RIGB presents many similarities with typical Archaean and Phanerozoic shear zone-hosted orogenic gold deposits. The features in common suggest similar processes in the formation of these deposits, irrespective of the geological time. The RIGB developed throughout ca 70 million years, between 2,152 and 2,080 Ma. The gold mineralisation succeeded the period of greater tectonic activity (2,130–2,080 Ma), occurring at a maximum of 30 million years after the peak of metamorphism (2,080 Ma) or, episodically, between 2,080 and 2,050 Ma.

Acknowledgements This study was sponsored by Fundação Coordenação de Aperfeiçoamento de Pessoal de Nível Superior - CAPES (Grant BEX0184/98-5). Analyses were carried out on a Sensitive High Resolution Ion Microprobe mass spectrometer (SHRIMP II) operated by a consortium consisting of Curtin University of Tecnology, the Geological Survey of Western Australia and the University of Western Australia with support from the Australian Research Council. We thank Dr. Léo Afraneo Hartmann and an anonymous referee for valuable comments on the paper.

References

Abouchami W, Boher M, Michard A, Albarède F (1990) A major 2.1 Ga event of mafic magmatism in West Africa: an early stage of crustal accretion. J Geophys Res 95:17605–17629

Åhäll KI, Cornell DH, Armstrong R (1998) Ion probe zircon dating of metasedimentary units across the Skagerrak: new constraints for Mesoproterozoic growth of the Baltic Shield. Precambrian Res 87:117–134

Aleinikoff JN, Graugh RI (1990) U–Pb geochronology constraints on the origin of a unique monazite-xenotime gneiss, Hudson Highlands, New York. Am J Sci 290:522–546

Alves da Silva FC (1994) Etude structurale du Greenstone belt Paleoproterozoique du Rio Itapicuru (Bahia, Brésil). Importance des granitoides syntectoniques, controle des mineralizations aurifères et evolution geodinamique transamazonienne (≈2.0 Ga) du Craton du São Francisco. Thèse de Doctorat, Université d'Orléans, France

Alves da Silva FC, Matos FMV (1991) Economic geology and structural controls of the orebodies from the Medium Itapicuru gold district: Rio Itapicuru grenstone belt, Bahia, Brazil. In: Ladeira EA (ed) Brazil Gold '91, Proceedings of Brazil Gold '91: the economics, geology, geochemistry and genesis of gold deposits. Balkema, Rotterdam, pp 629–635

Barrueto HR, Oliveira EP, Dallágnol R (1998) Trace element and Nd isotope evidence for juvenile, arc-related granitoids in the southern portion of the Paleoproterozoic Rio Itapicuru greenstone belt (RIGB), Bahia, Brazil. XL Congresso Brasileiro de Geologia, Belo Horizonte, Boletim de Resumos. BH, SBG-MG, pp 520

Brito Neves BB, Cordani UG, Torquato JRF (1980) Evolução geocronológica do Precambriano do Estado da Bahia. In: Geologia e Recursos Minerais do Estado da Bahia. Textos Básicos. Salvador, CPM-SME 3:1–101

Boher M, Abouchami W, Michard A, Albarède F, Arndt NT (1992) Crustal growth in West Africa at 2.1 Ga. J Geophys Res 97:345–369

Burgos CMG, Conceição H, Rios DC, Scheller T, Macambira MJB, Oliveira LL (1999) $^{207}Pb/^{206}Pb$ single zircon evaporation data of the agulhas and Bananas massif (Northeast Bahia State, Brazil). In: II South American Symposium on Isotope Geology, Cordoba, Argentina. Extended abstract, pp 19–22

Chauvet A, Guerrot C, Alves da Silva F, Faure M (1997) Géochronologie $^{207}Pb/^{206}Pb$ et $^{40}Ar/^{39}Ar$ des granites paléoprotérozoiques de la ceinture de roches vertes du Rio Itapicuru (Bahia, Brésil). CR Acad Sci Paris, 324, série Iia, 293–300

Coelho CES (1994) Genèse des fluides dans les ceinture de roches vertes de Rio Itapicuru (Brésil): Gisements de Fazenda Brasileiro et Fazenda Maria Preta. Une reconstitution basée sur l'étude des inclusions fluides dans leur contexte microstructural. Thèse de Doctorat, Université d'Orléans, France

Cumming GL, Richards JR (1975) Ore lead isotope ratios in a continuously changing earth. Earth Planet Sci Lett 28:155–171

Compston W, Willians IS, Meyer C (1984) U–Pb geochronology of zircons from lunar breccia 73217 using a sensitive high mass-resolution ion microprobe. Proceedings of the 14th Lunar and Planetary Science Coference. Part 2. J Geophys Res 89:B525–B534

Cumbest RJ, Johnson EL, Onstott TC (1994) Argon composition of metamorphic fluids: implications for $^{40}Ar/^{39}Ar$ geochronology. Geol Soc Amer Bull 106:942–951

Danilatos GD (1993) Introduction to the ESEM instrument. Microsc Res Tech 25:354–361

Davis DW, Hirdes W, Schaltegger U, Nunoo EA (1994) U–Pb age constraints on deposition and provenance of Birimian and gold-bearing Tarkwaian sediments in Ghana, West Africa. Precambrian Res 67:89–107

Davison I, Teixeira JBG, Silva MG, Rocha Neto MB, Matos FMV (1988) The Rio Itapicuru Greenstone Belt, Bahia, Brazil: structure and stratigraphical outline. Precambrian Res 42:1–17

Delor C, Egal E, Lafon JM, Cocherie A, Guerrot C, Rossi P, Truffert C, Théveniaut H, Phillips D, Avelar VG (2003) Transamazonian crustal growth and reworking as revealed by the 1: 500,000-scale geological map of French Guiana, 2nd edn. Géologie de la France, Orleans, pp 5–57

Eliasson T, Schöberg H (1991) U–Pb dating of the post-kinematic Sveconorwegian (Grevillian) Bohus granite, SW Sweden: evidence of restitic zircon. Precambrian Res 51:337–350

Feybesse JL, Milési JP (1994) The Archaean/Proterozoic contact zone in West Africa: a mountain belt of de´collement thrusting and folding on a continental margin related to 2.1 Ga convergence of Archaean cratons? Precambrian Res 69:199–227

Feybesse JL, Johan V, Triboulet C, Guerrot C, Mayaga-Mikolo F, Bouchot V, Eko N'dong J (1998) The West Central African belt: a model of 2.5–2.0 Ga accretion and two-phase orogenic evolution. Precmbrian Res 87:161–216

Gomes FCA, Kwitko RE, Nascimento HS (1998) Caracterização da seqüência meta-vulcanossedimentar e alteração hidrotermal associada na região de Lagoa do Gato, distrito aurífero de Fazenda Brasileiro—Ba. XL Congresso Brasileiro de Geologia, Boletim de Resumos, BH, SBG-MG, p 125

Griffin BJ (1997a) A new mechanism for the imaging of crystal structure in non-conductive materials: an application of charge-induced contrast in the environmental scanning electron microscope (ESEM). Proceedings Microscopy and Microanalysis 1997. Cleveland, Ohio, pp 1197–1198

Griffin BJ (1997b) Novel and advanced applications of the low vacuun and environmental scanning electron microscope (SEM). Proceedings Microscopy and Microanalysis 1997. Cleveland, Ohio, pp 385–386

Groves DI, Goldfarb RJ, Gebre-Mariam M, Hagemann SG, Robert F (1998) Orogenic gold deposits: a proposed classification in the context of their crustal distribution and relationship to other gold deposits types. Ore Geol Rev 13:7–27

Harrison TM, McDougall I (1985) Investigations of an intrusive contact, northwest Nelson, New Zeland-I thermal, chronological and isotopic constraints. Geochim Cosmochim Acta 44:1985–2003

Hartmann LA (2002) The Mesoproterozoic supercontinent Atlantica in the Brazilian Shield-review of geological and U_Pb zircon and Sm_Nd isotopic evidence. Gondwana Res 5:157–163

Heaman LM, Parrish RR (1991) U–Pb geochronology of acessory minerals. In: Heaman L, Ludden JN (eds) Application of Radiogenic isotope system to problems in geology. Short Course Handb 19:59–102

Hirdes W, Davis DW (2002) U–Pb geochronology of Paleoproterozoic rocks in the southern part of the Kedougou-Ke´nie´ba Inlier, Senegal, West Africa: evidence for diachronous accretionary development of the Eburnean province. Precambrian Res 118:83–99

Hirdes W, Davis DW, Eisenlohr BN (1992) Reassessment of Proterozoic granitoid ages in Ghana on the basis of U–Pb zircon and monazite dating. Precambrian Res 56:89–96

Hirdes W, Davis DW, Lüdtke G, Konan G (1996) Two generations of Birimian (Paleoproterozoic) volcanic belts in northeastern Côte d'Ivoire (West Africa): consequences for the 'Birimian controversy'. Precambrian Res 80:173–191

Kamber BS, Frei R, Gibb AJ (1998) Pitfalls and new approaches in granulite chronometry. An example from the Limpopo Belt, Zimbabwe. Precambrian Res 91:269–285

Kinny PD (1997) Users guide to U–Th–Pb dating of titanite, perovskite, monazite and baddeleyite using W. A. SHRIMP. W. A. Isotope Science Research Centre, School of Physical Sciences, Curtin University of Technology, Perth, Australia. Report no. SPS693119971AP72, p 21

Kinny PD, Nutman AP (1996) Zirconology of the Meeberrie gneiss, Yilgarn Craton, Western Australia: an early Archaean migmatite. Precambrian Res 78:165–178

Kishida A, Riccio L (1980) Chemostratigraphy of lava sequences from the Itapicuru greenstone belt, Bahia, Brazil. Precambrian Res 11:161–178

Lacerda CMM, Oliveira EP (1997) Características texturais de deformação e segregação magmática no domo de Ambrósio, Greenstone Belt do Rio Itapicuru, Bahia. In: SBG, Simpósio Nacional de Estudos Tectônicos, 7 Lençois, Boletim de Estudos Expandidos, seção V, pp 49–51

Ledru P, Johan V, Milési JP, Tegyey M (1994) Markers of the last stages of the Palaeoproterozoic collision: evidence for a 2 Ga continent involving circum-South Atlantic provinces. Precambrian Res 69:169–191

Marimon MPC, Kishida A, Teixeira JBG (1986) Estudo da alteração hidrotermal relacionada à mineralização aurífera na Fazenda Brasileiro (Ba): 34 Congresso Brasileiro de Geologia, Goiania. Anais Soc Bras Geologia 4:1556–1570

Matos FMV, Davison I (1987) Basement or intrusion? The Ambrósio dome, Rio Itapicuru greenstone belt, Bahia, Brazil. International symposium on granites and associated mineralization, Salvador, Bahia, Brazil, vol 14, n 4, pp 442–449

McDougall I, Harrison TM (1988) Geochronology and thermochronology of the $^{40}Ar/^{39}Ar$ Method. Oxford University Press, Oxford, p 212

Mcnaughton NJ, Rasmussen B, Fletcher IR (1999) SHRIMP uranium–lead dating of diagenetic xenotime in siliciclastic sedimentary rocks. Science 285:78–80

Milési JP, Lerouge C, Delór C, Ledru P, Billa M, Cocherie A, Egal E, Fouillac AM, Lahondère D, Lasserre JL, Marot A, Martel-Jantin B, Rossi P, Tegyey M, Théveniaut H, Thiéblemont D, Vanderhaeghe O (2003) Gold deposits (gold-bearing tourmalinites, gold-bearing conglomerates, and mesothermal lodes), markers of the geological evolution of French Guiana: geology, metallogeny, and stable-isotope constraints. Géologie de la Francen. 2-3-4, pp 257–290

Mello EF, Assis CM, Orlandi PH, Costa CHC, Albuquerque R, Silva GLP, Xavier RP (1996) Contribuição à tipologia dos veios auríferos da Mina Fazenda Brasileiro, BA. XXXIX Congresso Brasileiro de Geologia, Salvador, Bahia, Boletim de Resumos, pp 238–241

Mello EF, Oliveira EP, McNaughton NJ (1999) SHRIMP U–Pb geochronology of early Precambrian quartzite and its basement (Caldeirão Belt), NE São Francisco Craton, Bahia, Brazil. In: II South American symposium on isotope geology, Cordoba, Argentina. Extended abstract, pp 78–81

Melo JRG (1990) Geochemical investigation of the hydrothermal alteration zone surrounding the greenstone-hosted Fazenda Brasileiro gold deposit, Bahia, Brazil. Ph.D. thesis, Colorado School of Mines, pp 574

Montes Lopes CA (1982) Algumas características geológicas e geoquímicas das mineralizações de ouro na área da jazida de Fazenda Brasileiro—Bahia. Dissertação de mestrado, Universidade Federal da Bahia, Salvador, pp 98

Nascimento HS, Gomes FCA, Kwitko R (1998) Caracterização petrográfica do granitóide tonalítico de Teofilándia-Greenstone belt do Rio Itapicuru, Bahia. XL Congresso Brasileiro de Geologia, Belo Horizonte, Boletim de Resumos, BH, SBG-MG, pp 502

Nelson DR (1997) Compilation of SHRIMP U–Pb zircon geochronology data, 1996. Geol Surv West Aust Rec 1997 (2):189

Norcross CE, Davis DW, Spooner ETC, Rust A (2000) U–Pb and Pb–Pb age constraints on Paleoproterozoic magmatism, deformation and gold mineralization in the Omai area, Guyana Shield. Precambrian Res 102:69–86

Oberthür T, Vetter U, Davis DW, Amanor JA (1998) Age constraints on gold mineralization and Paleoproterozoic crustal evolution in the Ashanti belt of southern Ghana. Precambrian Res 89:129–143

Oliveira LL, Rios DC, Burgos CMG, Conceição H, Macambira MJB, Santos CGP, Scheller T (1999) Geochronology of Cansanção Massif by $^{207}Pb/^{206}Pb$ evaporation method, Northeastern of Bahia State, Brazil. In: II South American Symposium on Isotope Geology, Cordoba, Argentina. Extended abstract, pp 90–93

Oliveira EP, Mello EF, McNaughton NJ (2002) SHRIMP U-Pb geochronology of early Precambrian quartzite and its basement (Caldeirão Belt), NE São Francisco Craton, Bahia, Brazil. J South Am Earth Sci 15:349–362

Peixoto AA, Rios DC, Scheller T, Macambira MJB, Conceição H (1999) New geochronological data of Morro dos Lopes granites, Serrinha Nucleus (Northeast Bahia State, Brazil). In: II South American Symposium on Isotope Geology, Cordoba, Argentina. Extended abstract, pp 98–100

Pidgeon RT (1992) Recrystallisation of oscillatory zoned zircon: some geochronological and petrological implications. Contrib Mineral Petrol 110:463–472

Pidgeon RT, Wilde SA (1998) The interpretation of complex zircon U–Pb systems in Archaean granitoids and gneisses from the Jack Hills, Narryer Gneiss Terrane, Western Australia. Precambrian Res 91:309–332

Pidgeon RT, Furfaro D, Kennedy AK, Nemchim AA, Bronswjk V (1994) Calibration of zircon standards for the Curtin SHRIMP II: Abstracts of the 8th International Conference on Geochronology, Cosmochronology and Isotope Geology, Berkeley, USA, U.S. Geological Survey Circular, 1107, pp 251

Plint HE, Mcdonough MR (1995) $^{40}Ar/^{39}Ar$ and K–Ar age constraints on shear zone, northeastern Alberta. Can J Earth Sci 32:181–191

Reinhardt MC, Davison I (1990) Structural and lithologic controls on gold deposition in the shear zone-hosted Fazenda Brasileiro mine, Bahia State, northeast Brazil. Econ Geol 85:952–967

Rios DC, Conceição H, Scheller T, Macambira MJB, McReath I, Conceição RV, Burgos CMG (1999) General aspects, geochemical and isotopic constraints on Morro do Afonso syenitic pluton, Northeastern Bahia, Brazil. In: II South American Symposium on Isotope Geology, Cordoba, Argentina. Extended abstract, pp 268–271

Rocha Neto MB (1994) Geologia e recursos minerais do *greenstone belt* do Rio Itapicuru, Bahia: In: Pedreira AJ (ed) Série Arquivos Abertos 4, CBPM, pp 32

Sabaté P, Caenvachette M, Marinho MM, Vidal, Soares Filho CP (1990) Dados isotópicos Rb/Sr e Sm/Nd da intrusão monzonítica a 2.0 Ga de Cansanção (Bahia, Brasil) implicações sobre as fontes. In: Cong. Bras de Geol, 36, Natal. Boletim de Resumos, Natal, SBG, p 163

Seth B, Kröner A, Mezger K, Nemchin AA, Pidgeon RT, Okrusch M (1998) Archaean to Neoproterozoic events in the Kaoko belt of NW Namibia and their geodynamic significance. Precambrian Res 92:341–363

Silva MG (1984) A sequência vulcano-sedimentar do médio Rio Itapicurú, Bahia: caracterização petrográfica, considerações petrogenéticas preliminares e zoneografia metamórfica. In: Sá PVSV, Duarte FB (eds), Geologia e Recursos Minerais do Estado da Bahia, Textos Básicos. Sec Minas e Energia, Salvador, pp 6–42

Silva MG (1987) Geochemie, Petrologie und geotektonische Entwicklung eines proterozoischen Gruensteinguertels: Rio Itapicuru, Bahia, Brasilien. Ph.D. Thesis, Freiburg University, Germany

Silva MG (1992) Evidências istópicas e geocronológicas de um fenômeno de acrescimento crustal Transamazônico, no Cráton de São Francisco, Estado da Bahia. Vol 2. Anais XXXVII Congresso Brasileiro de Geologia Boletim de Resumos, São Paulo, SBG, p 182

Smith JB, Barley ME, Groves DI, Krapez B, Mcnaughton NJ, Bickle MJ, Chapman HJ (1998) The sholl shear zone, West Pilbara: evidence for a domain boundary structure from integrated tectonostratigraphic analyses, SHRIMP U–Pb dating and isotopic and geochemical data of granitoids. Precambrian Res 88:143–171

Snee LW, Sutter JF, Kelly WC (1988) Thermochronology of economic mineral deposits: dating the stages of mineralization at Panasqueira, Portugal, by high-precision $^{40}Ar/^{39}Ar$ age spectrum techniques on muscovite. Econ Geol 83:335–354

Taylor PN, Moorbath S, Leube A, Hirdes W (1992) Early Proterozoic crustal evolution in the Birimian of Ghana: constraints from geochronology and isotope geochemistry. Precambrian Res 56:97–111

Teixeira JBG (1985) Geologia e controles da mineralização aurífera em Fazenda Brasileiro, Serrinha (BA). In: Sá PVSV, Duarte FB (eds) Geologia e recursos minerais do Estado da Bahia: Textos básicos. Salvador, Brasil, Secretaria das Minas e Energia 6:9–49

Teixeira JBG, Kishida A, Marimon MPC, Xavier RP, Mcreath I (1990) The Fazenda Brasileiro gold deposit, Bahia: geology hydrothermal alteration, and fluid inclusion studies. Econ Geol 85:990–1009

Vasconcelos P, Becker T (1992) A idade da mineralização aurífera no depósito da Fazenda Brasileiro, Bahia, Brasil. Workshop em Metalogênese: Pesquisas atuais e novas tendências.UNICAMP, Boletim de Resumos, p 29

Wetherill GW (1956) Discordant uranium lead ages. Trans Amer Geophys Union 37:320–326

Willians LS (1992) Some observations on the use of zircon U–Pb geochronology in the study of granitic rocks. Trans R Soc Edinburgh Earth Sci 83:447–458

Willians LS, Claesson S (1987) Isotopic evidence for the Precambrian provenance and Caledonian metamorphism of high grade paragneisses from the Seve Nappes, Scandinavian caledonides.II.Ion microprobe zircon U–Th–Pb. Contrib Mineral Petrol 97:205–217

Xavier RP (1987) Estudo de inclusões fluidas na mina de ouro Fazenda Brasileiro, greenstone belt do Rio Itapicuru, Bahia: Tese de Mestrado, Universidade de São Paulo, São Paulo

Xavier RP (1991) The role of microstructural and fluid process in the genesis of gold-bearing shear zones: Fazenda Maria mine, Rio Itapicuru greenstone belt, Bahia, Brazil. Ph.D. thesis, University of Southampton, UK

Xavier RP (1994) Fluidos associados a depósitos de ouro mesotermais do Greenstone Belt do Rio Itapicuru, Bahia: Principais características e possíveis fontes. SIMP CSF II, Salvador, Anais Salvador, SBG/SGM 1:319–322

Xavier RP, Foster RP (1991) The role of carbonaceous shear bands in fluid-flow and gold-precipitation inn the Fazenda Maria Preta mine, Bahia, northeast Brazil. In: Ladeira EA (ed). Proceedings of Brazil Gold '91: the Economics, Geology, Geochemistry and Genesis of Gold Deposits. Balkema, Rotterdam, pp 269–277

Xavier RP, Foster RP, Fallick AE, Alderton DHM (1994) Potential fluids reservoirs for mesothermal gold deposit in the Rio Itapicuru greenstone belt, Bahia, Brazil. Comunicaciones, Univ de Chile 45:13–22

Yamana Gold INC (2005) Yamana Gold INC home page. http://www.yamana.com. Cited 22 Sept 2005

Zhao G, Cawood PA, Wilde SA, Sun M (2002) Review of global 2.1–1.8 Ga orogens: implications for a pre-Rodinia supercontinent. Earth Sci Rev 59:125–162